Computational Methodology Study of the Optical and Thermochemical Properties of a Molecular Photoswitch

ARTICLE *in* THE JOURNAL OF PHYSICAL CHEMISTRY A · JANUARY 2015

Impact Factor: 2.69 · DOI: 10.1021/jp510678u · Source: PubMed

10 AUTHORS, INCLUDING:

Jonas Elm
University of Copenhagen
19 PUBLICATIONS **138** CITATIONS
SEE PROFILE

Mogens Brøndsted Nielsen
University of Copenhagen
132 PUBLICATIONS **2,076** CITATIONS
SEE PROFILE

Henrik G Kjaergaard
University of Copenhagen
141 PUBLICATIONS **3,817** CITATIONS
SEE PROFILE

Kurt V Mikkelsen
University of Copenhagen
266 PUBLICATIONS **6,541** CITATIONS
SEE PROFILE

THE JOURNAL OF PHYSICAL CHEMISTRY A

Article

pubs.acs.org/JPCA

Computational Methodology Study of the Optical and Thermochemical Properties of a Molecular Photoswitch

Stine T. Olsen, Jonas Elm,* Freja Eilsø Storm, Aske Nørskov Gejl, Anne S. Hansen, Mia Harring Hansen, Jens Rix Nikolajsen, Mogens Brøndsted Nielsen, Henrik G. Kjaergaard, and Kurt V. Mikkelsen

Department of Chemistry, H. C. Ørsted Institute, University of Copenhagen, Universitetsparken 5, DK-2100 Copenhagen, Denmark

Supporting Information

ABSTRACT: We assess how the utilization of different DFT functionals for obtaining the equilibrium geometries and vibrational frequencies affect the description of the thermochemistry and subsequent calculation of the optical properties of a dihydroazulene−vinylheptafulvene photoswitch. The assessment covers nine popular DFT functionals (BLYP, B3LYP, CAM-B3LYP, M06-L, M06, M06-2X, PBE, PBE0, and ωB97X-D) in conjugation with five different Pople style basis sets (6-31+G(d), 6-31++G(d,p), 6-311+G(d), 6-311++G(d,p), and 6-311++G(3df,3pd)). It is identified that only CAM-B3LYP, M06-2X, and PBE0 are able to quantitatively describe the correct trends in the thermochemical properties. The subsequent calculation of the optical properties using the CAM-B3LYP functional shows that there is little difference in whether the CAM-B3LYP, M06-2X, or PBE0 functionals have been used to calculate the equilibrium geometries. Utilizing the identified functionals, we investigate how the number of electron withdrawing cyano substituents influence the thermochemistry and optical properties of the molecular photoswitch.

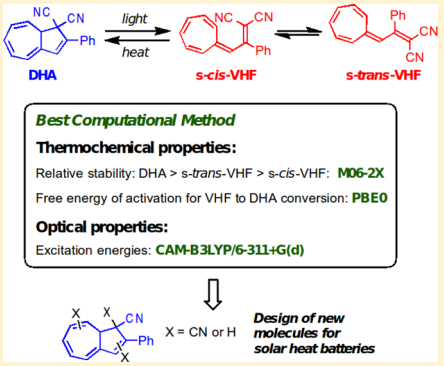

1. INTRODUCTION

The term molecular photoswitch is used to describe a molecular switch, which interconverts reversibly between at least two different states with the stimulus of light. Photoswitches have been extensively studied with moieties including azobenzene,[1] diarylethene,[2,3] and spiropyran.[4,5] The photochromic dihydroazulene (DHA) derivatives, first introduced by Daub et al. in 1984, are a fascinating group of compounds, which can undergo photoinduced ring-opening to form vinylheptafulvenes (VHF),[6] which in turn can undergo a thermally induced ring-closure back to DHA, Figure 1. The ring-opening reaction occurs with a high quantum yield,[7,8] whereas the back-reaction is relatively slow. Thus, the DHA/VHF photoswitch shows promising application as a molecular energy storage device[9] and has also been the subject of numerous synthesis work for creating candidate derivatives for molecular electronics.[10−12] DHA is particularly interesting in the context of solar heat batteries because the absorption maximum is around 350 nm, which corresponds to a high intensity in the solar flux, whereas VHF is absorbing in the visible region with a maximum absorption around 470 nm. The nonphotoactive absorption of VHF has been shown to be influenced systematically by solvent,[7,13] with a red shift in absorption maximum with increasing solvent polarity. The quantum yield and maximum absorption of DHA is also influenced by solvent, but no systematic behavior has been reported.[7,8,14] The switching properties of the DHA/VHF system have been attempted to be tuned by attachment of either electron donating groups or withdrawing groups.[7,8,15−18] Studies have shown a correlation between functionalization and rate of back-reaction,[7] and the effect of functionalization on the seven-membered ring with regard to the VHF to DHA conversion is opposite to that of the five-membered ring.

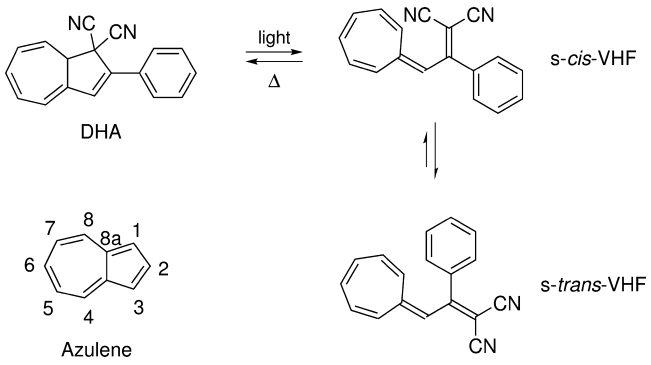

Figure 1. DHA/VHF photoswitch. The initial product of the ring-opening is the VHF in its *s-cis* conformation, from where it rotates into its more stable *s-trans* conformation through thermal equilibrium.

Theoretical investigations using quantum mechanics are a promising tool for identifying potential rational design strategies[19] and can greatly reduce the amount of work needed for synthesizing new target compounds. A popular choice for calculating molecular properties is density functional theory (DFT). Previously, theoretical investigations include the

Received: October 24, 2014
Revised: December 30, 2014
Published: January 8, 2015

DOI: 10.1021/jp510678u
J. Phys. Chem. A 2015, 119, 896−904

functionals B3LYP, PBE0, CAM-B3LYP, and ωB97X-D.[19,20] For the application of using the DHA/VHF system as energy storage devices, we herein investigate how the utilization of different DFT functionals affect the thermochemical and optical properties of the DHA/VHF photoswitch system. Ideally, the chosen functional should yield a more stable DHA structure than VHF, the Enthalpy of activation of the back-reaction $\Delta H_{VHF\rightarrow TS}$ should be in the range 18−21 kcal/mol depending on the solvent,[7] and the functional should be able to yield the correct excitation energy of the system, i.e., ∼350 nm for DHA and ∼470 nm for VHF. The investigated functional includes BLYP, B3LYP, CAM-B3LYP, M06-L, M06, M06-2X, PBE, PBE0, and ωB97X-D with a wide range of Pople style basis sets. Finally, for improving the molecular structure for application in solar energy storage devices, the effect of number and placement of cyano groups (CN) is addressed.

2. COMPUTATIONAL METHODOLOGY

All density functional theory calculations have been performed in Gaussian 09.[21] Explicitly correlated coupled cluster results have been performed in MOLPRO.[22] We test a series of DFT functionals (BLYP,[23,24] B3LYP,[25,26] CAM-B3LYP,[27] M06-L,[28] M06,[29] M06-2X,[29] PBE,[30] PBE0,[31,32] and ωB97X-D[33]) with varying HF-exchange and inherent different constructions in conjugation with five Pople style basis sets: 6-31+G(d), 6-31++G(d,p), 6-311+G(d), 6-311++G(d,p), and 6-311++G(3df,3pd) for optimizing the geometry and calculating the vibrational frequencies. The optimizations are in all cases the equilibrium geometry of the ground state (S_0). The correlation consistent basis sets (cc-pVXZ and aug-cc-pVXZ, X = D, T) were also tested, but the inclusion of diffuse functions yielded severe convergence issues and thereby they were neglected in the analysis. Applying all combinations of the DFT functionals and basis sets allows the investigation of the importance of HF-exchange, long-range correction, dispersion correction, and basis set convergence for several important properties of the systems such as the relative thermochemical stability of DHA/VHF and excitation energies. For calculating the vertical excitation energies, we exclusively use the CAM-B3LYP functional, which has shown adequate performance for a variety of organic systems in recent benchmarks.[34,35] Furthermore, the CAM-B3LYP functional has also previously been successfully employed in the calculation of various response properties such as polarizabilities,[36,37] absorption,[38,39] van der Waals C_6-coefficients,[36] and natural[40−42] and magnetic circular dichroism.[43−45] Solvent effects are taken into account using a polarizable continuum model with the integral equation formalism variant (IEFPCM) as implemented in Gaussian.[46,47] In all cases where a solvent has been applied, both the equilibrium geometry/frequencies and subsequent calculation of the excitation energies have been performed using IEFPCM. All solvent calculations of free energies include the zero point vibrational energy and thermal contributions and are evaluated at 298.15 K. For the solvent calculations two different solvents were tested with high difference in polarity: cyclohexane and acetonitrile. Absorption spectra are simulated using Gaussian line shapes with a peak half-width at half-maximum of 0.33 eV as implemented in GaussView 5.0.[48]

3. SENSITIVITY ANALYSIS OF APPLIED DFT METHODS

3.1. Structure Sampling. Due to internal rotations, the DHA and VHF structures were initially sampled using a systematic rotator approach as implemented in Avogadro.[49] The identified 11 rotamers of DHA and 119 rotamers of VHF were initially geometry optimized using the B3LYP/6-31+G(d) level of theory, which narrowed down the conformations to one distinct DHA, one *s-trans*-VHF and two *s-cis*-VHF conformations. The transition states for the photoinduced ring-opening reaction were manually searched and verified as a first-order saddle point with a single imaginary frequency, which corresponds to the vibration along the breaking bond. In Figure 2, the identified molecular structures of DHA, VHF, and the transition state (TS) calculated at the B3LYP/6-31+G(d) level of theory can be seen. These identified structures were then used as the starting point for the following thermochemical analysis.

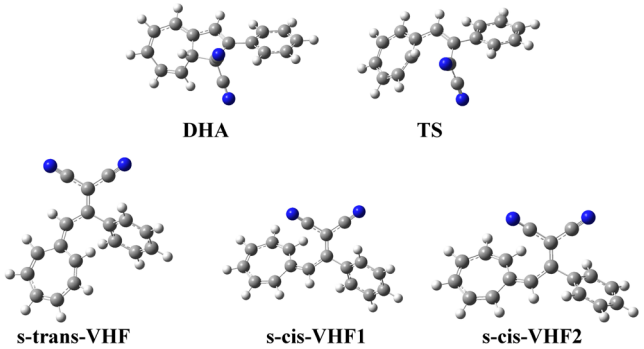

Figure 2. Identified molecular structures of dihydroazulene (DHA), vinylheptafulvene (VHF), and the transition state (TS) for the transformation between DHA and VHF.

3.2. Assessment of Thermochemical Properties. In Table 1 the stability of DHA relative to VHF ($\Delta G_{DHA} - \Delta G_{VHF}$, i.e., a negative value means that DHA is more stable than VHF) as well as the barrier height for the back-reaction $\Delta H_{VHF\rightarrow TS}$ of the *s-cis*-VHF to DHA are shown in a vacuum (vac), cyclohexane (ch), and acetonitrile (an), calculated for all the functionals, presented using the 6-31+G(d) basis set.

It is observed (in a vacuum) that only CAM-B3LYP, M06, M06-2X, and PBE0 correctly predict the relative stability $\Delta G_{DHA} < \Delta G_{VHF}$, with varying stabilities of 4.2, 2.1, 6.5, and 4.1 kcal/mol, respectively. As a comparison, a DF-LCCSD(T)-F12a/VDZ//MP2/6-31+G(d) calculation was performed, which predicts a value of −7.9 kcal/mol for the relative stability. This indicates that the M06-2X functional yields the relative stability in best agreement with higher level *ab initio* results with a discrepancy of only 1.4 kcal/mol. The inclusion of solvent effects flips the stability for the ωB97X-D functional such that DHA is more stable than VHF for both cyclohexane and acetonitrile. The opposite trend is observed for the M06 functional, where the inclusion of solvent in the case of acetonitrile flips the stability such that VHF is more stable than DHA. Generally, as the polarity of the solvent is increased, the stability of DHA relative to VHF is reduced. In the case of the CAM-B3LYP and PBE0 functionals the stabilities in acetonitrile are seen to be more or less identical. For several derivatives it has been shown experimentally that DHA is more stable than VHF[7] and the thermal conversion of VHF to DHA occurs

DOI: 10.1021/jp510678u
J. Phys. Chem. A 2015, 119, 896−904

Table 1. Relative ΔG of DHA/VHF and the ΔH Barrier for the Back-Reaction *s-cis*-VHF → TS in a Vacuum (vac), Cyclohexane (ch), and Acetonitrile (an)[a]

method	$\Delta G_{DHA} - \Delta G_{VHF}$(vac)	$\Delta H_{VHF \rightarrow TS}$(vac)	$\Delta G_{DHA} - \Delta G_{VHF}$(ch)	$\Delta H_{VHF \rightarrow TS}$(ch)	ΔG_{DHA} - ΔG_{VHF}(an)	$\Delta H_{VHF \rightarrow TS}$(an)
BLYP	7.6	20.8	9.4	19.9	12.3	20.0
B3LYP	2.7	23.2	4.7	22.3	7.3	20.9
CAM-B3LYP	−4.2	25.9	−2.7	24.4	0.0	21.2
M06-L	3.6	23.4	5.2	21.9	8.1	21.7
M06	−2.1	28.8	−0.4	23.0	2.7	19.7
M06-2X	−6.5	26.1	−5.4	24.9	−3.6	23.0
PBE	1.1	19.1	2.9	18.7	2.6	17.6
PBE0	−4.1	22.1	−2.4	21.3	0.3	19.0
ωB97X-D	7.6	24.8	−5.2	23.8	−2.4	21.4
exp						∼18−21[7]

[a]All values are calculated using the 6-31+G(d) basis set and presented in kcal/mol.

always quantitatively. The only functional that covers this trend over the range of solvents is the M06-2X functional. All the functionals did independently of basis set and solvent correctly depict the *s-trans*-VHF conformation to be more stable than the *s-cis*-VHF.

The barrier for the back-reaction of VHF to DHA is seen to be directly dependent on the amount of exact HF-exchange for each family of functionals, such that BLYP < B3LYP < CAM-B3LYP and PBE < PBE0 and M06-L < M06 < M06-2X for the Minnesota type functionals. For most functionals a slight overestimation is observed, but overall, a good agreement with the experimental values of ∼18−21 kcal/mol depending on solvent is observed.

The thermochemical properties are found to only be faintly dependent on the basis set utilized in the geometry optimization and frequency calculation; see Supporting Information. All functionals show similar trends: as the basis set is increased, the relative stability of DHA to VHF is decreased. This leads to a slight increase in the barrier of the back-reaction of VHF to DHA. For all functionals the dependence on the basis set size utilized for the geometry optimization and the subsequent frequency calculation accounts for less than 1 kcal/mol in the corresponding thermochemistry. This indicates that utilizing the smaller 6-31+G(d) basis set for obtaining the structure and frequencies yield equal functionalization as the large polarized Pople basis set 6-311++G(3df,3pd). It should, however, be noted that an error of the order of 1 kcal/mol would imply a significant percent-wise error for several of the functionals reported in Table 1. Using the ωB97X-D functional with a triple-ζ basis set yielded spurious results for the barrier of the back-reaction, where an increase from 24.78 to 35.77 kcal/mol was observed when the basis set was increased from 6-31+G(d) to 6-311+G(d). The origin of this discrepancy was identified to be purely due to the empirical dispersion term, as a similar trend was not observed when utilizing the ωB97X functional instead of ωB97X-D. From these findings it appears that M06-2X would yield the most reliable relative free energies of DHA and VHF, whereas PBE0 yields the best agreement with the experimental data of the back-reaction of VHF to DHA.

3.3. Convergence of Optical Properties. Besides the thermochemical properties of the molecular photoswitching reaction, an adequate description of the optical properties is also important. The first three excitation energies have been calculated using CAM-B3LYP with the basis sets 6-31G, 6-31+G(d), 6-31++G(d,p), 6-311G, 6-311+G(d), 6-311++G-(d,p), and 6-311++G(3df,3pd) for each of the geometries identified from above. From vacuum calculations some general trends in basis set convergence can be established. See the Supporting Information for more details. It should be noted that the following use of the term λ_{max} corresponds to the excitation energy with the highest oscillator strength. It is observed that within each basis set, the λ_{max} value gets blue-shifted with increasing HF-exchange incorporated in the functional utilized for the geometry optimization such that λ_{max}(CAM-B3LYP//BLYP) > λ_{max}(CAM-B3LYP//B3LYP) > λ_{max}(CAM-B3LYP//CAM-B3LYP). Similarly, it is observed in the case of the Minnesota family of functionals with λ_{max}(CAM-B3LYP//M06-L) > λ_{max}(CAM-B3LYP//M06) > λ_{max}(CAM-B3LYP//M06-2X) and for λ_{max}(CAM-B3LYP//PBE) > λ_{max}(CAM-B3LYP//PBE0). This shift can be as high as 25 nm depending on functional. The basis set utilized in the geometry optimization accounts for a blue shift of up to 4−7 nm in the λ_{max} value when the basis set was increased from 6-31+G(d) to 6-311+G(d). The inclusion of an additional set of diffuse functions on hydrogens or further polarized functions up to (3df,3pd) in the geometry optimization does not change the subsequent calculation of the excitation energy.

For the calculation of the excitation energies, the inclusion of the first set of diffuse/polarized functions from 6-31G → 6-31+G(d) or 6-311G → 6-311+G(d) is very important and corresponds to a red shift of 7−19 nm in the λ_{max} values. The inclusion of a set of diffuse/polarized functions on hydrogen is seen to have a negligible effect. Increasing the basis set from a double-ζ to a triple-ζ when calculating the excitation energies only yields a slight difference of 1−3 nm in the λ_{max} value. Similarly, it is observed that the amount of polarized functions is increased when calculating the excitation energy with a variation of around 1−2 nm when increasing from 6-311++G(d,p) to 6-311++G(3df,3pd). On the basis of these findings, we can conclude that the utilization of a 6-311+G(d) basis set for the geometry optimization/frequency calculation and also the 6-311+G(d) basis set for subsequently calculating of the excitation energies is sufficient to yield converged values.

3.4. Test of the Chosen Methodology. The 15 lowest excitation energies have been calculated using CAM-B3LYP/6-311+G(d) for each of the functionals which described the thermochemistry trends correctly (CAM-B3LYP, M06-2X, and PBE0). In Figure 3, the effect of using different functionals for optimizing the equilibrium geometry on the optical properties can be seen for DHA, depicted in cyclohexane.

It is observed that the spectral features are insensitive to the choice of functional used to optimize the geometry, Table 2. The lowest electronic transitions have an oscillator strength in

DOI: 10.1021/jp510678u
J. Phys. Chem. A 2015, 119, 896−904

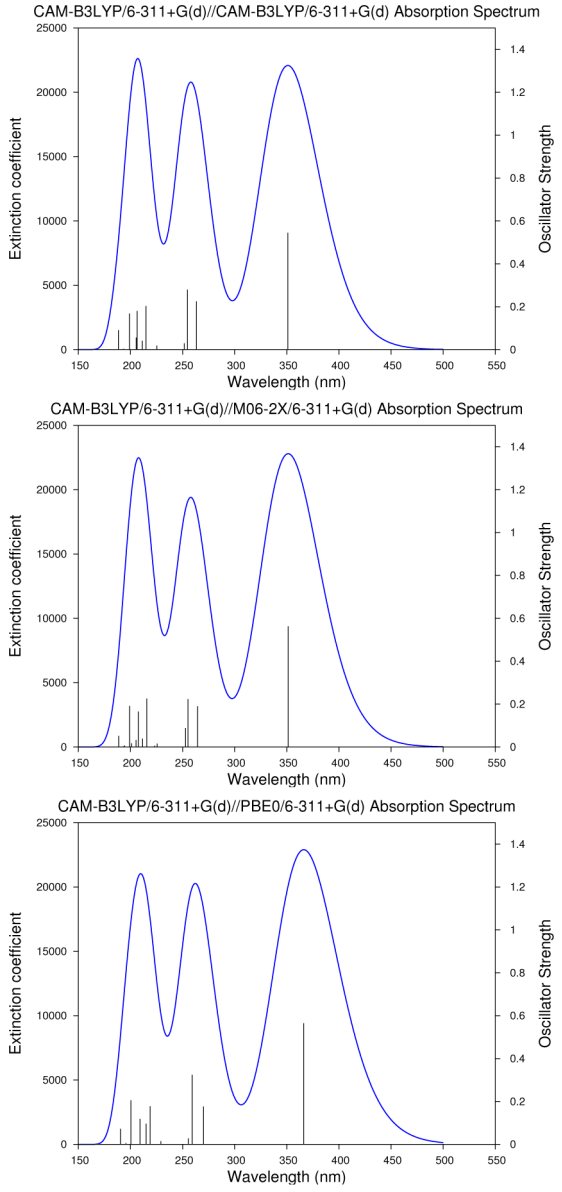

Figure 3. Simulated absorption spectrum (HWHM = 0.33 eV) at the CAM-B3LYP/6-311+G(d) level of theory for the lowest identified Gibbs free energy structure of DHA with three different functionals utilized for optimizing the geometry in cyclohexane. The extinction coefficient is given in L mol^{-1} cm^{-1}. Top: CAM-B3LYP/6-311+G(d) geometry. Middle: M06-2X/6-311+G(d) geometry. Bottom: PBE0/6-311+G(d) geometry.

Table 2. CAM-B3LYP/6-311+G(d) Calculated Excitation Energies (nm) in Cyclohexane for the Three Functionals Which Described the Thermochemical Trends Correctly[a]

	DHA	*s-trans*-VHF	*s-cis*-VHF1	*s-cis*-VHF2
//CAM-B3LYP	351 (0.55)	425 (0.88)	434 (0.55)	429 (0.64)
//M06-2X	351 (0.56)	424 (0.87)	434 (0.52)	429 (0.62)
//PBE0	366 (0.56)	442 (0.66)	451 (0.56)	444 (0.65)
exp	354	446		

[a]Oscillator strengths are given in parentheses.

the range 0.55−0.57. Using the CAM-B3LYP or M06-2X functional for optimizing the geometry leads to a maximum absorption occurring at 351 nm, whereas PBE0 leads to a

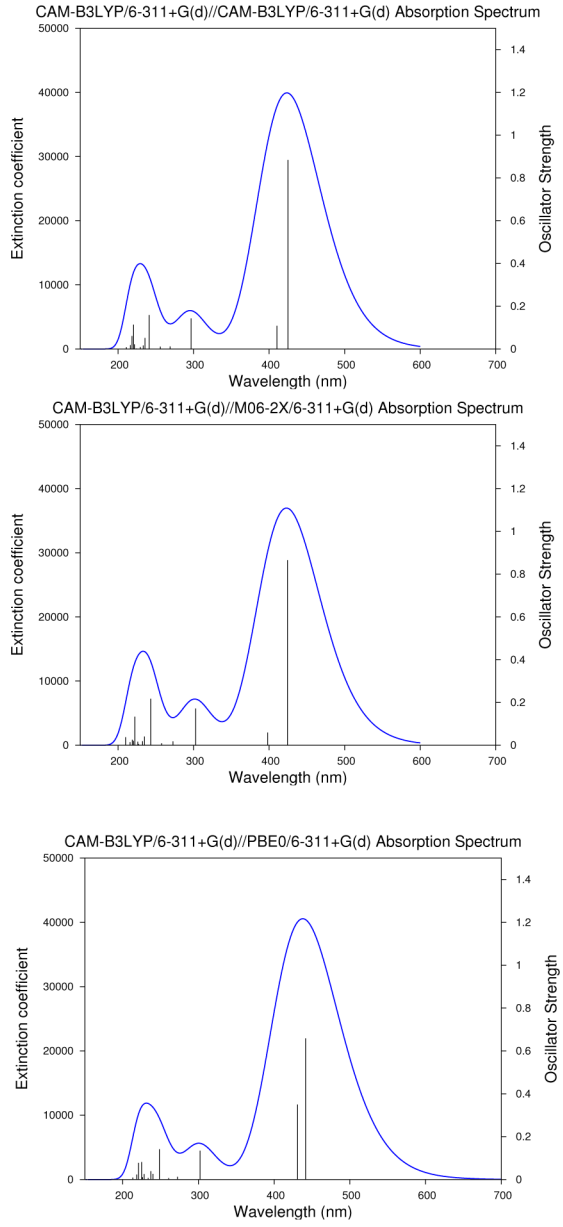

Figure 4. Simulated absorption spectrum (HWHM = 0.33 eV) at the CAM-B3LYP/6-311+G(d) level of theory for the lowest identified Gibbs free energy structure of VHF with three different functionals utilized for optimizing the geometry in cyclohexane. The extinction coefficient is given in L mol^{-1} cm^{-1}. Top: CAM-B3LYP/6-311+G(d) geometry. Middle: M06-2X/6-311+G(d) geometry. Bottom: PBE0/6-311+G(d) geometry.

maximum absorption of 366 nm. These values are in relatively good agreement with the experimental value of DHA in cyclohexane of 354 nm.[13] In Figure 4 the effect of using different functionals for optimizing the equilibrium geometry on the optical properties can be seen for the lowest identified Gibbs free energy conformation of VHF, depicted in cyclohexane.

Similarly to DHA, the overall spectral features are independent of the functional used for optimizing the geometry. Variation in the calculated oscillator strengths are observed. This does, however, not influence the extinction coefficient, which in all three cases is close to 40 000 L mol^{-1} cm^{-1} independent of the functionals. The maximum absorption

DOI: 10.1021/jp510678u
J. Phys. Chem. A 2015, 119, 896−904

wavelength is seen to vary from 425 nm in the case where M06-2X and CAM-B3LYP have been used to optimize the geometry, up to 442 nm with PBE0. In all three cases this is a slight blue shift compared to the experimental value of 446 nm.[13] Because three different VHF conformations were identified during the structural sampling, it is important to investigate how the different conformations affect the absorption spectrum. In Figure 5, the simulated absorption spectrum of the identified *s-trans*-VHF and two *s-cis*-VHF conformations can be seen at the CAM-B3LYP/6-311+G(d) level of theory. The three conformations have the relative Gibbs free energies of 0.00, 1.98, and 3.49 kcal/mol, respectively.

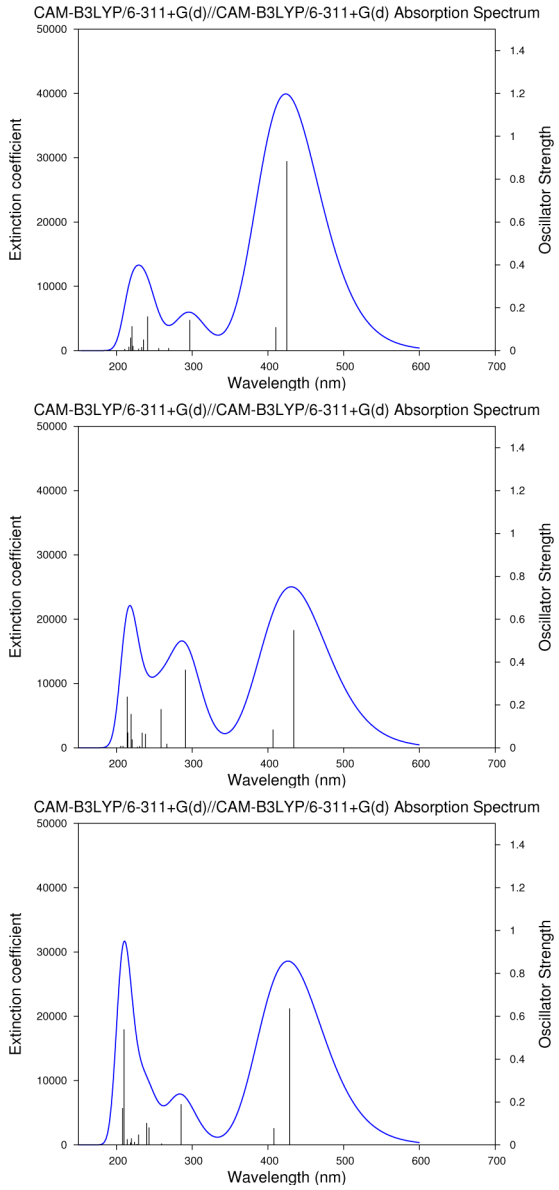

Figure 5. Simulated absorption spectrum (HWHM = 0.33 eV) at the CAM-B3LYP/6-311+G(d)//CAM-B3LYP/6-311+G(d) level of theory for the three different identified VHF conformations in cyclohexane. The extinction coefficient is given in L mol^{-1} cm^{-1}. Top: *s-trans*-VHF. Middle: *s-cis*-VHF1. Bottom: *s-cis*-VHF2. Relative stabilities of 0.00, 1.98, and 3.49 kcal/mol, respectively.

It is observed that the *s-trans* conformation yields a significantly larger extinction coefficient than the *s-cis* conformations, increased from ~30 000 to over 40 000 L mol^{-1} cm^{-1}. The overall spectral features are consistent for all three conformations, with a strong band in the visible region and two small bands in the UV region. Because the *s-trans* conformation is more stable than the *s-cis* conformers by 1.98 kcal/mol or more, it can be assumed that the thermally averaged spectrum will highly represent that of the *s-trans* conformation, with a slight contribution from the *s-cis* conformations to the spectral features in the UV region.

From these combined findings it can be seen that the spectral features of the DHA-VHF photoswitch system is rather independent of the functional used for optimizing the geometry. The maximum absorption wavelength of DHA is well reproduced compared to experiment, and we observe a slight blue shift in the calculated VHF maximum absorption wavelength. It is thereby seen that no single DFT functional is capable of describing both the thermochemistry and optical properties correctly, and hereby the utilization of several functionals are recommended.

4. SUBSTITUENT EFFECT

4.1. Substituent Effect on the Thermochemical Properties. With the DHA/VHF as a candidate for advanced devices, many attempts have been made by tuning the properties of the system. For applications related to solar energy storage, the maximum absorption near solar flux and high storage capability, i.e., high $\Delta G_{DHA} - \Delta G_{VHF}$, are important challenges.

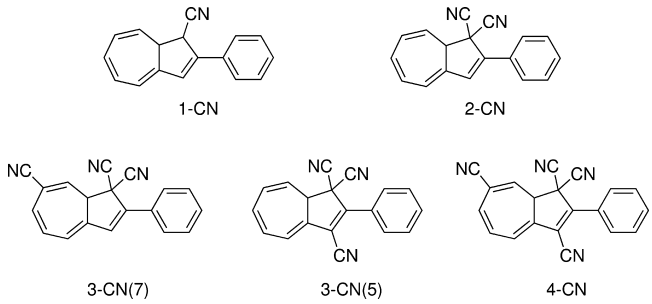

Figure 6. Investigated DHA structures with one to four CN substituents. The number in brackets refers to functionalization in the five- or seven-membered ring.

Experimentally, Daub and co-workers have focused on the functionalization of the five-membered ring in position 3,[7,8] whereas later Nielsen and co-workers have developed a method for studying the influence of placing a substituent in the seven-membered ring in position 7.[50] However, the synthetic work is time-consuming, which hereby motivates a theoretical study. To investigate the number and placement of up to four CN groups, we decided to study the five different structures given in Figure 6.

For all five identified molecular structures a systematic structural sampling was performed similarly to section 3.1, except that after the initial B3LYP/6-31+G(d) screening the geometry optimization was performed only with CAM-B3LYP, M06-2X, and PBE0 functionals with the 6-311+G(d) basis set. In the case of the 1-CN-DHA compound the *R,R*-diastereoisomer was found lowest in free energy and was thereby employed in all the following calculations.

In Table 3, the relative stability of DHA/VHF ($\Delta G_{DHA} - \Delta G_{VHF}$) and barrier for the back-reaction ($\Delta H_{VHF \rightarrow TS}$) can be

DOI: 10.1021/jp510678u
J. Phys. Chem. A 2015, 119, 896−904

Table 3. Relative ΔG of DHA/VHF with One to Four Cyano Substituents and the ΔH Barrier for the Back-Reaction *s-cis*-VHF → TS in a Vacuum (vac), Cyclohexane (ch), and Acetonitrile (an)[a]

method	$\Delta G_{DHA} - \Delta G_{VHF}$(vac)	$\Delta H_{VHF \rightarrow TS}$(vac)	$\Delta G_{DHA} - \Delta G_{VHF}$(ch)	$\Delta H_{VHF \rightarrow TS}$(ch)	$\Delta G_{DHA} - \Delta G_{VHF}$(an)	$\Delta H_{VHF \rightarrow TS}$(an)
			1CN			
CAM-B3LYP	−12.5	31.1	−12.5	30.6	−12.5	30.1
M06-2X	−13.8	30.4	−13.7	29.9	−14.0	29.7
PBE0	−14.0	25.6	−13.7	25.3	−13.7	25.0
			2CN			
CAM-B3LYP	−3.8	26.1	−2.5	24.5	0.1	21.1
M06-2X	−6.6	26.1	−5.4	24.8	−3.8	22.8
PBE0	−4.1	22.1	−2.5	21.2	0.2	18.8
			3CN (on 7 Ring)			
CAM-B3LYP	−4.3	28.0	−3.4	27.0	−2.4	25.0
M06-2X	−6.5	27.8	−5.9	27.2	−4.8	25.6
PBE0	−4.8	23.1	−4.0	22.5	−2.4	21.3
			3CN (on 5 Ring)			
CAM-B3LYP	−4.2	25.7	−2.4	25.2	0.5	25.5
M06-2X	−6.3	25.8	−4.4	25.8	−1.8	26.2
PBE0	−4.8	21.7	−3.0	22.0	0.5	23.5
			4CN			
CAM-B3LYP	−4.8	29.1	−3.6	28.5	−1.5	27.4
M06-2X	−6.7	28.8	−5.5	28.5	−3.2	27.8
PBE0	−5.6	24.5	−4.2	24.2	−1.9	24.0

[a]All values are calculated using the 6-311+G(d) basis set and presented in kcal/mol.

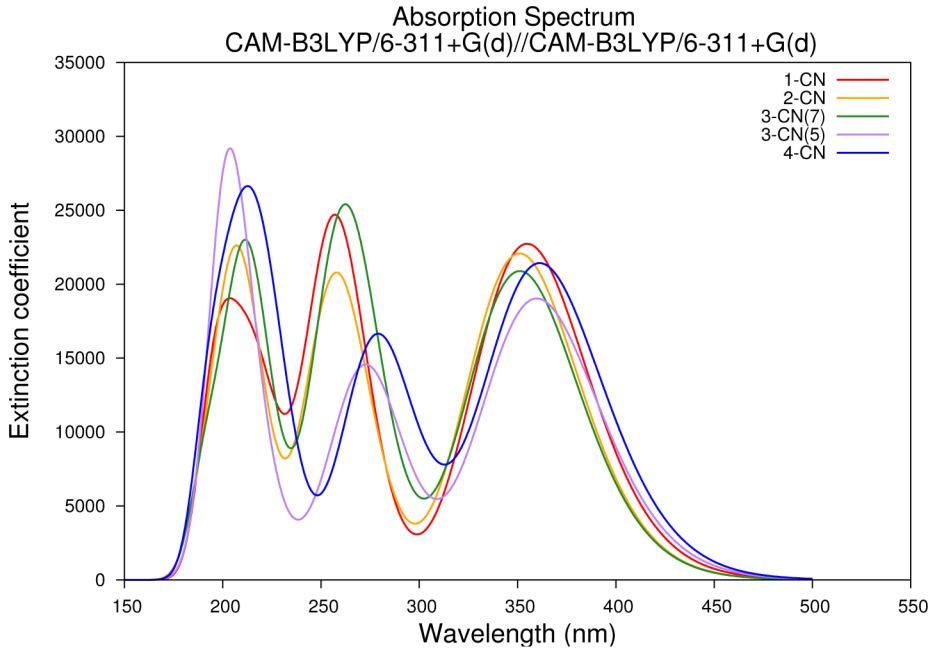

Figure 7. Simulated absorption spectrum at the CAM-B3LYP/6-311+G(d)//CAM-B3LYP/6-311+G(d) level of theory for DHA with either 1-, 2-, 3-, or 4-CN groups in cyclohexane. The extinction coefficient is given in L mol^{-1} cm^{-1}.

Table 4. Maximum Absorption (nm) Wavelength of the Substituted DHA and VHF Derivatives Calculated at the CAM-B3LYP/6-311+G(d)//CAM-B3LYP/6-311+G(d) Level of Theory in Cyclohexane

	λ_{max}^{DHA}	λ_{max}^{VHF1}	$\Delta\lambda_{VHF-DHA}$
1-CN	355 (0.56)	375 (0.76)	20
2-CN	351 (0.55)	425 (0.88)	74
3-CN(5)	360 (0.47)	429 (0.37)	69
3-CN(7)	351 (0.52)	398 (0.75)	47
4-CN	361 (0.53)	387 (0.34)	26

seen for the derivatives with one, two, three, or four cyano groups. For all the utilized functionals in a vacuum, it is seen that the relative stability of DHA/VHF is rather independent of whether there are two, three, or four CN groups attached to the molecular framework with stabilities within 1 kcal/mol. Increasing the polarity of the solvent is seen to decrease the relative stability. A large increase in the relative stability is observed in the DHA-1CN/VHF-1-CN system. This is due to the DHA-1-CN structure being stabilized compared to the VHF-1CN, attributed to a decreasing strain in the five- and seven-membered rings compared to the 2-CN-, 3-CN, and 4-

DOI: 10.1021/jp510678u
J. Phys. Chem. A 2015, 119, 896−904

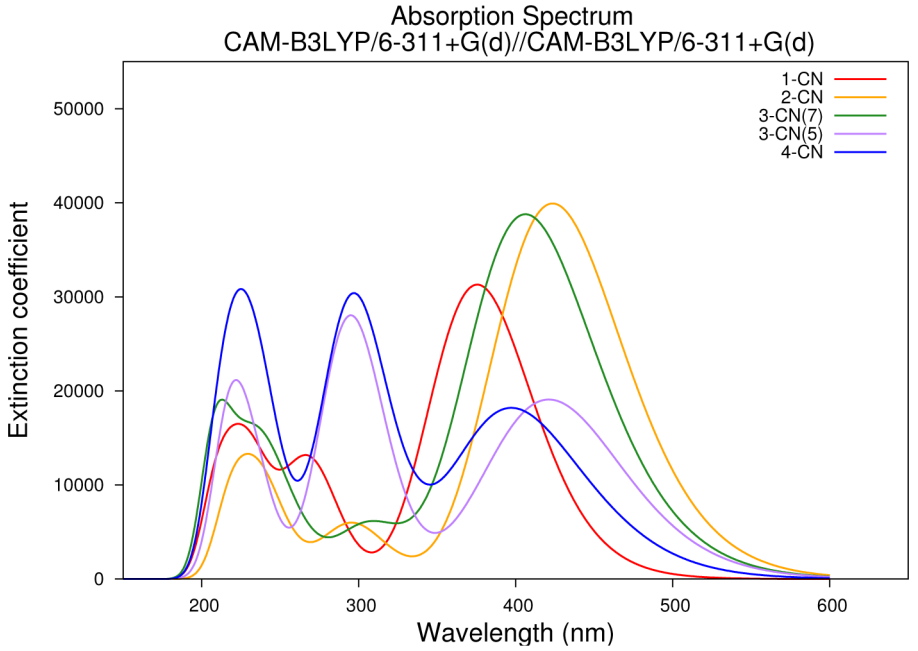

Figure 8. Simulated absorption spectrum at the CAM-B3LYP/6-311+G(d)//CAM-B3LYP/6-311+G(d) level of theory for VHF with either 1-, 2-, 3-, or 4-CN groups in cyclohexane. The extinction coefficient is given in L mol^{-1} cm^{-1}.

CN analogues. For the application of energy storage, a single cyano group could thereby be desirable in position 1. Interestingly, it is found in the case of the 4-CN and 3-CN(5-ring) derivatives that the *s-cis* conformation is more stable than the *s-trans*-conformation. This is attributed to the *s-trans* conformation being destabilized by the addition of the cyano group to the five-membered ring due to sterical hindrance.

The back-reaction is, besides the storage capability, an important factor for use in solar heat batteries, because the stored energy should be able to be released. The back-reaction from *s-cis*-VHF to DHA is seen to be affected by the added substituents. From the vacuum calculations the barrier height of the back-reaction follows the following pattern: 1-CN > 4-CN > 3-CN(7) > 2-CN > 3-CN(5). Thereby, only the derivative with the third cyano group positioned at the five-membered ring has a decreased barrier height compared to that of the parent 2-CN compound. The barrier of the back-reaction is observed to be solvent dependent, with varying effect depending on the functional and number of cyano groups. For the 1-CN derivatives there is observed almost no dependence on solvent, with the back-reaction only decreasing ∼1 kcal/mol when changing from a vacuum to acetonitrile. There is observed a slightly higher influence of solvent on the back-reactions of the 3-CN and 4-CN derivatives, with a variation of 2−3 kcal/mol, when changing from a vacuum to acetonitrile. From the general trend it can be seen that for the application of solar energy storage, the surrounding medium should be as apolar as possible, to ensure a high reaction barrier for the VHF → DHA conversion.

4.2. Substituent Effect on the Optical Properties. With the hope of a future utilization of the DHA/VHF system in solar heat batteries, it is crucial to find DHA derivatives that absorb light at a wavelength corresponding to a high solar flux. In Figure 7, the absorptions of the five derivatives of DHA are depicted. All derivatives are observed to have absorption maxima in the region 351−361 nm, Table 4; however, with the exception of 1-CN, a red small shift is observed for an increased number of CN groups, 2-CN < 3-CN(7) < 1-CN < 3-CN(5) < 4-CN, thereby providing a larger overlap with the actinic flux. Interestingly, it was found that the absorption maximum is more red-shifted for functionalization of the five-membered ring compared to that of the seven-membered ring, which is opposite to the thermodynamic properties. On the basis of these calculations, substitution of more electron withdrawing groups on the five-membered ring like CN could therefore be interesting for future investigations, or a stronger electron withdrawing group could be used for further red-shifting the absorption.

The VHF absorption can be used to probe the switching reaction, and Figure 8 depicts the spectra for all five derivatives. It is observed that the absorption maximum is blue-shifted for the 1-, 3-, and 4-CN compared to the case of the 2-CN VHF, with a significantly larger blue shift for the 1-CN VHF. Comparing 2-CN versus 3-CN(7) with 3-CN-(5) versus 4-CN, we observe that a CN group at the seven-membered ring will blue-shift the absorption maximum, whereas a CN group at the corresponding DHA at the five-membered ring will increase the intensity of the absorption. Thus, the effect of the number and placement of electron withdrawing groups is larger on the VHF structure than on the DHA structure. However, it should be noted that the $\Delta\lambda_{\text{VHF-DHA}}$ value, Table 4, is particular low for 1-CN and 4-CN, which might make it difficult to see the switching using UV−vis spectroscopy. However, Raman spectroscopy of the CN groups might be useful in this case.[51]

5. CONCLUSIONS

We have investigated the utilization of nine different DFT functionals with varying basis sets for obtaining the equilibrium geometries, the vibrational frequencies, the thermochemistry, and the optical properties of dihydroazulene−vinylheptafulvene photoswitches. Calculations were performed both in a vacuum and in the solvents cyclohexane and acetonitrile. From the thermochemical analysis, it was found that only the functionals

DOI: 10.1021/jp510678u
J. Phys. Chem. A 2015, 119, 896−904

of CAM-B3LYP, M062X, and PBE0 correctly predicted the thermochemical trends, where M062X yielded the most reliable free energies of DHA and VHF, whereas the PBE0 functional yielded the best agreement with experimental data of the back-reaction. The thermochemical properties only slightly depended on basis set i.e less than 1 kcal/mol, and it was found that the 6-311+G(d) basis set was sufficient.

The analysis of the optical properties was performed with the long-range corrected CAM-B3LYP functional on the different geometry optimized structures. It was found that within each basis set the λ_{max} value got blue-shifted with increased HF-exchange incorporated in the functional utilized for the geometry optimization, as high as 25 nm depending on functional. However, regarding the CAM-B3LYP, M062X, and PBE0 functionals, the spectral features were rather independent of the functional used for geometry optimization. The excitation energies are found to depend on basis set. The inclusion of the first set of diffuse functions is significant and accounts for a red shift of 7−19 nm in the λ_{max} values, whereas the inclusion of a set of diffuse functions on the hydrogen seemed to have a negligible effect. We identify that the 6-311+G(d) basis set was sufficient to yield converged optical properties.

As a future candidate for solar heat batteries, the thermochemical and the optical properties of DHA/VHF have been tried tuned by theoretically varying the number and placements of CN groups in the system. The 1-CN-DHA/1-CN-VHF system, in which a CN at position 1 of DHA has been substituted with an H, was found to have a significantly larger relative stability than the 2-CN, 3-CN, and 4-CN systems, thus leading to a significant higher energy storage. The back-reaction barrier was only lowered by the third cyano group positioned at the five-membered ring compared to the parent DHA with two CN groups, whereas the 1-CN system had the highest barrier. With the exception of 1-CN a red shift in λ_{max} value was observed for an increase in the number of CN groups, where the strongest red shift is observed for functionalization of the five-membered ring. Subsequent work should thereby be focusing on the 1-CN-DHA derivative.

■ ASSOCIATED CONTENT

Supporting Information

The excitation energies and thermochemical and optical properties employing different functionals and basis set are available as Supporting Information. This material is available free of charge via the Internet at http://pubs.acs.org/.

■ AUTHOR INFORMATION

Corresponding Author

*J. Elm. E-mail: elm@chem.ku.dk.

Notes

The authors declare no competing financial interest.

■ ACKNOWLEDGMENTS

The authors thank the Danish Center for Scientific Computing for providing computer resources, and the Danish Natural Science Research Council/The Danish Councils for Independent Research, and the Center for Exploitation of Solar Energy founded by the University of Copenhagen for financial support.

■ REFERENCES

(1) Hartley, G. S. The Cis-form of Azobenzene. *Nature* **1937**, *140*, 281−281.
(2) Irie, M.; Mohri, M. Thermally Irreversible Photochromic Systems - Reversible Photocyclization of Diarylethene Derivatives. *J. Org. Chem.* **1988**, *53*, 803−808.
(3) Irie, M. Diarylethenes for Memories and Switches. *Chem. Rev.* **2000**, *100*, 1685−1716.
(4) Fischer, E.; Hirschberg, Y. *J. Chem. Soc.* **1952**, 4522−4524.
(5) Berkovic, G.; Krongauz, V.; Weiss, V. Spiropyrans and Spirooxazines for Memories and Switches. *Chem. Rev.* **2000**, *100*, 1741−1753.
(6) Daub, J.; Knochel, T.; Mannschreck, A. Photosensitive Dihydroazulenes with Chromogenic Properties. *Angew. Chem., Int. Ed.* **1984**, *23*, 960−961.
(7) Görner, H.; Fisher, C.; Gierisch, S.; Daub, J. Dihydroazulene Vinaylheptafulvene Photochromism - Effects of Substituents, Solvent, and Temperature in the Photorearrangement of Dihydroazulenes to Vinylheptafulvenes. *J. Phys. Chem.* **1993**, *97*, 4110−4117.
(8) Görner, H.; Fisher, C.; Daub, J. Photoreaction Dihydroazulenes Into Vinylheptafulvenes - Photochromism of Nitrophenyl-Substituted Derivatives. *J. Photochem. Photobiol., A* **1995**, *85*, 217−224.
(9) Kucharski, T. J.; Tian, Y.; Akbulatov, S.; Boulatov, R. Chemical Solutions for the Closed-cycle Storage of Solar Energy. *Energy Environ. Sci.* **2011**, *4*, 4449−4472.
(10) Lara-avila, S.; Danilov, A. V.; Kubatkin, S. E.; Broman, S. L.; Parker, C. R.; Nielsen, M. B. Light-Triggered Conductance Switching in Single-Molecule Dihydroazulene Vinylheptafulvene Junctions. *J. Phys. Chem. C* **2011**, 18372−18377.
(11) Broman, S. L.; Lara-Avila, S.; Thisted, C. L.; Bond, A. D.; Kubatkin, S.; Danilov, A.; Nielsen, M. B. Dihydroazulene Photoswitch Operating in Sequential Tunneling Regime: Synthesis and Single-Molecule Junction Studies. *Adv. Funct. Mater.* **2012**, *22*, 4249−4258.
(12) Broman, S. L.; Jevric, M.; Bond, A. D.; Nielsen, M. B. Syntheses of Donor Acceptor-Functionalized Dihydroazulenes. *J. Org. Chem.* **2014**, *79*, 41−64.
(13) Broman, S. L.; Brand, S. L.; Parker, C. R.; Petersen, M. A.; Tortzen, C. G.; Kadziola, A.; Kilså, K.; Nielsen, M. B. Optimized Synthesis and Detailed NMR Spectroscopic Characterization of the 1,8a-Dihydroazulene-1,1-dicarbonitrile Photoswitch. *Arkivoc* **2011**, 51−67.
(14) Feringa, B. L. *Molecular Switches*; Wiley: New York, 2001.
(15) Broman, S. L.; Petersen, M. A.; Tortzen, C. G.; Kilså, K.; Kadziola, A.; Nielsen, M. B. Arylethynyl Derivatives of the Dihydroazulene/Vinylheptafulvene Photo/Thermoswitch: Tuning the Switching Event. *J. Am. Chem. Soc.* **2010**, *132*, 9165−9174.
(16) Petersen, M. Å.; Broman, S. L.; Kadziola, A.; Kilså, K.; Nielsen, M. B. Gaining Control: Direct Suzuki Arylation of Dihydroazulenes and Tuning of Photo- and Thermochromism. *Eur. J. Org. Chem.* **2011**, *6*, 1033−1039.
(17) Gierisch, S.; Bauer, W.; Burgemeister, T.; Daub, J. Substituents Dependency of the Dihydroazulene-Reversible-Vinylheptafulvene Photochromism - Steric and Electronic Effects of 9-Anthryl Compounds - New Access to Condensed Hydropentalenes. *Chem. Ber.* **1989**, *122*, 2341−2349.
(18) Schalk, O.; Broman, S. L.; Petersen, M. A.; Khakhulin, D. V.; Brogaard, R. Y.; Nielsen, M. B.; Boguslavskiy, A. E.; Stolow, A.; Sølling, T. I. On the Condensed Phase Ring-Closure of Vinylheptafulvalene and Ring-Opening of Gaseous Dihydroazulene. *J. Phys. Chem. A* **2013**, *117*, 3340−3347.
(19) Shahzad, N.; Nisa, R. U.; Ayub, K. Substituents Effect on Thermal Electrocyclic Reaction of Dihydroazulene-Vinylheptafulvene Photoswitch: a DFT Study To Improve the Photoswitch. *Struct. Chem.* **2013**, *24*, 2115−2126.
(20) Perrier, A.; Maurel, F.; Jacquemin, D. Diarylethene-Dihydroazulene Multimode Photochrome: A Theoretical Spectroscopic Investigation. *Phys. Chem. Chem. Phys.* **2011**, *13*, 13791−13799.
(21) Frisch, M. J.; Trucks, G. W.; Schlegel, H. B.; Scuseria, G. E.; Robb, M. A.; Cheeseman, J. R.; Scalmani, G.; Barone, V.; Mennucci,

DOI: 10.1021/jp510678u
J. Phys. Chem. A 2015, 119, 896−904

B.; Petersson, G. A.; et al. *Gaussian 09*, Revision B.01; Gaussian, Inc.: Wallingford, CT, 2010.
(22) Werner, H.-J.; Knowles, P. J.; Knizia, G.; Manby, F. R.; Schütz, M.; et al. *MOLPRO*, version 2012.1, a package of ab initio programs; http://www.molpro.net.
(23) Becke, A. D. Density-Functional Exchange-Energy Approximation with Correct Asymptotic Behavior. *Phys. Rev. A* **1988**, *23*, 3098−3100.
(24) Lee, C.; Yang, W.; Parr, R. G. Development of the Colle-Salvetti Correlation-Energy Formula into a Functional of the Electron Density. *Phys. Rev. B* **1988**, *37*, 785−789.
(25) Stephens, P. J.; Devlin, F. J.; Chabalowski, C. F.; Frisch, M. J. Ab Initio Calculation of Vibrational Absorption and Circular Dichroism Spectra Using Density Functional Force Fields. *J. Phys. Chem.* **1994**, *98*, 11623−11627.
(26) Becke, A. Density-Functional Thermochemistry. III. The Role of Exact Exchange. *J. Chem. Phys.* **1993**, *98*, 5648−5652.
(27) Yanai, T.; Tew, D. P.; Handy, N. C. A New Hybrid Exchange-Correlation Functional using the Coulomb-Attenuating Method (CAM-B3LYP). *Chem. Phys. lett.* **2004**, *393*, 51−57.
(28) Zhao, Y.; Truhlar, D. G. A New Local Density Functional for Main-Group Thermochemistry, Transition Metal Bonding, Thermochemical Kinetics, and Noncovalent Interactions. *J. Chem. Phys.* **2006**, *125*, 94101:1−18.
(29) Zhao, Y.; Truhlar, D. G. The M06 Suite of Density Functionals for Main Group Thermochemistry, Thermochemical Kinetics, Noncovalent Interactions, Excited States, and Transition Elements: Two New Functionals and Systematic Testing of Four M06-Class Functionals and 12 other Functionals. *Theor. Chem. Acc.* **2008**, *120*, 215−241.
(30) Perdew, J. P.; Burke, K.; Ernerhof, M. Generalized Gradient Approximation Made Simple. *Phys. Rev. Lett.* **1996**, *77*, 3865−3868.
(31) Ernzerhof, M.; Scuseria, G. E. Assessment of the Perdew-Burke-Ernzerhof Exchange-Correlation Functional. *J. Chem. Phys.* **1999**, *110*, 5029−5036.
(32) Adamo, C.; Barone, V. Toward Reliable Density Functional Methods without Adjustable Parameters: The PBE0 Model. *J. Chem. Phys.* **1999**, *110*, 6158−6170.
(33) Chai, J.; Head-Gordon, M. Long-Range Corrected Hybrid Density Functionals with Damped Atom-Atom Dispersion Corrections. *Phys. Chem. Chem. Phys.* **2008**, *10*, 6615−6620.
(34) Jacquemin, D.; Wathelet, V.; Pertéte, E. A.; Adamo, C. Extensive TD-DFT Benchmark: Singlet-Excited States of Organic Molecules. *J. Chem. Theory Comput.* **2009**, *5*, 2420−2435.
(35) Jacquemin, D.; Mennucci, B.; Adamo, C. Excited-State Calculations with TD-DFT: From Benchmarks to Simulation in Complex Environments. *Phys. Chem. Chem. Phys.* **2011**, *13*, 16987−16998.
(36) Kauczor, J.; Norman, P.; Saidi, W. A. Non-Additivity of Polarizabilities and van der Waals C6 Coefficients of Fullerenes. *J. Chem. Phys.* **2013**, *138*, 114107.
(37) Limacher, P. A.; Mikkelsen, K. V.; Lüthi, H. P. On the Accurate Calculation of Polarizabilities and Second Hyperpolarizabilities of Polyacetylene Oligomer Chains using the CAM-B3LYP Density Functional. *J. Chem. Phys.* **2009**, *130*, 194114.
(38) Lind, P.; Carlsson, M.; Eliasson, B.; Glimsdal, E.; Lindgren, M.; Lopes, C.; Boman, L.; Norman, P. A Theoretical and Experimental Study of Non-Linear Absorption Properties of Substituted 2,5-Di-(phenylethynyl)thiophenes and Structurally Related Compounds. *Mol. Phys.* **2009**, *107*, 629−641.
(39) Westerlund, F.; Elm, J.; Lykkebo, J.; Carlsson, N.; Thyrhaug, E.; Åkerman, B.; Sørensen, T. J.; Mikkelsen, K. V.; Laursen, B. W. Direct Probing of Ion Pair Formation Using a Symmetric Triangulenium Dye. *Photochem. Photobiol. Sci.* **2011**, *10*, 1963−1973.
(40) Jiemchooroj, A.; Norman, P. X-ray Absorption and Natural Circular Dichroism Spectra of C84: A Theoretical Study using the Complex Polarization Propagator Approach. *J. Chem. Phys.* **2008**, *128*, 234304.
(41) Elm, J.; Lykkebo, J.; Sørensen, T. J.; Laursen, B. W.; Mikkelsen, K. V. Racemization Mechanisms and Electronic Circular Dichroism of [4]Heterohelicenium Dyes: A Theoretical Study. *J. Phys. Chem. A* **2011**, *115*, 12025−12033.
(42) Elm, J.; Lykkebo, J.; Sørensen, T. J.; Laursen, B. W.; Mikkelsen, K. V. Obtaining Enhanced Circular Dichroism in [4]Heterohelicenium Analogues. *J. Phys. Chem. A* **2012**, *116*, 8744−8752.
(43) Solheim, H.; Ruud, K.; Coriani, S.; Norman, P. Complex Polarization Propagator Calculations of Magnetic Circular Dichroism Spectra. *J. Chem. Phys.* **2008**, *128*, 094103.
(44) Fahleson, T.; Kauczor, J.; Norman, P.; Coriani, S. The Magnetic Circular Dichroism Spectrum of the C-60 Fullerene. *Mol. Phys.* **2013**, *111*, 1401−1404.
(45) Santoro, F.; Improta, R.; Fahleson, T.; Kauczor, J.; Norman, P.; Coriani, S. Relative Stability of the L_a and L_b Excited States in Adenine and Guanine: Direct Evidence from TD-DFT Calculations of MCD Spectra. *J. Phys. Chem. Lett.* **2014**, *5*, 1806−1811.
(46) Miertus, S.; Scrocco, E.; Tomasi, J. Electrostatic Interaction of a Solute with a Continuum. A Direct Utilization of ab initio Molecular Potentials for the Prevision of Solvent Effects. *Chem. Phys.* **1981**, *55*, 117−129.
(47) Tomasi, J.; Mennucci, B.; Cammi, R. Quantum Mechanical Continuum Solvation Models. *Chem. Rev.* **2005**, *105*, 2999−3093.
(48) Dennington, R.; Keith, T.; Millam, J. *GaussView* Version 5; Semichem Inc.: Shawnee Mission, KS, 2009.
(49) Hanwell, M. D.; Curtis, D. E.; Lonie, D. C.; Vandermeersch, T.; Zurek, E.; Hutchison, G. R. Avogadro: An advanced semantic chemical editor, visualization, and analysis platform. *J. Cheminf.* **2012**, 4−17.
(50) Petersen, M. Å.; Broman, S. L.; Kadziola, A.; Kilså, K.; Nielsen, M. B. Dihydroazulene Photoswitches: The First Synthetic Protocol for Functionalizing the Seven-Membered Ring. *Eur. J. Org. Chem.* **2009**, 2733−2736.
(51) Li, T.; et al. Ultrathin Reduced Graphene Oxide Films as Transparent Top-Contacts for Light Switchable Solid-State Molecular Junctions. *Adv. Mater.* **2013**, *25*, 4164−4170.

DOI: 10.1021/jp510678u
J. Phys. Chem. A 2015, 119, 896−904